The Extended Discrete Element Method (XDEM) for Multi-Physics Applications

Bernhard Peters

Abstract

The Extended Discrete Element Method (XDEM) is a novel numerical simulation technique that extends the dynamics of granular materials or particles as described through the classical discrete element method (DEM) by additional properties such as the thermodynamic state, stress/strain, or electromagnetic field for each particle coupled to a continuum phase such as fluid flow or solid structures. Contrary to a continuum mechanics concept, XDEM aims at resolving the particulate phase through the various processes attached to particles. While DEM predicts the spacial-temporal position and orientation for each particle, XDEM additionally estimates properties such as the internal temperature and/or species distribution. These predictive capabilities are further extended by an interaction to fluid flow by heat, mass and momentum transfer and impact of particles on structures. These superior features as compared to traditional and pure continuum mechanic approaches are highlighted by predicted examples of relevant engineering applications.

1 Introduction

Numerous engineering applications include physics from multiple domains, and not just a single domain; these are referred to as multi-physics. In such cases, as long as the phenomena considered are to be treated by either a continuous, i.e., Eulerian, or discrete, i.e., Lagrangian, approach, a homogeneous numerical solution may be employed to solve the problem. However, there exist other engineering applications that simultaneously include both a continuous and a discrete phase, and therefore, they cannot be solved accurately by continuous or discrete approaches alone. In particular, a discrete approach to determine both the dynamic (position and orientation) and thermodynamic (temperature and species) states of individual and discrete particles of an ensemble has not yet been developed. Similarly, the impact of particles on the structure or flow of gases or liquids has largely remained unexplored.

Numerical approaches to model multi-phase flow phenomena including a solid e.g. particulate phase may basically be classified into two categories: All phases are treated as a continuum on a macroscopic level of which the two fluid model is the most well-known representative (Gidaspow, 1994). It is well suited to two-phase modelling due to its computational convenience and efficiency. However, all the data concerning size distribution, shape or material properties of individual particles is lost to a large extent due to the averaging concept. Therefore, this loss of information on small scales has to be compensated for by additional constitutive or closure relations.

An alternative approach considers the solid phase as discrete, while the flow of liquids or gases is treated as a continuum phase in the void space between the particles, and therefore, is labelled the Combined Continuum and Discrete Model (CCDM) (Tsuji et al., 1993; Hoomans et al., 1996; Xu and Yu, 1997, 1998). Due to a discrete description of the solid phase, constitutive relations are omitted, and therefore, leads to a better understanding of the fundamentals. This was also concluded by Zhu et al. (Zhu et al., 2007) and Zhu et al. (Zhu et al., 2008) during a review on

particulate flows modelled with the CCDM approach. It has seen a mayor development in last two decades and describes motion of the solid phase by the Discrete Element Method (DEM) on an individual particle scale and the remaining phases are treated by the Navier-Stokes equations. Thus, the method is recognized as an effective tool to investigate into the interaction between a particulate and fluid phase as reviewed by Yu and Xu (Yu and Xu, 2003), Feng and Yu (Feng and Yu, 2004) and Deen et al. (Deen et al., 2007).

Initially, such studies are limited to simple flow configurations (Hoomans et al., 1996; Tsuji et al., 1993), however, Chu and Yu (Chu and Yu, 2008) demonstrated that the method could be applied to a complex flow configuration consisting of a fluidized bed, conveyor belt and a cyclone. Similarly, Zhou et al. (Zhou et al., 2011) applied the CCDM approach to the complex geometry of fuel-rich/lean burner for pulverised coal combustion in a plant and Chu et al. (Chu et al., 2009) modelled the complex flow of air, water, coal and magnetite particles of different sizes in a dense medium cyclone (DMC). For both cases re-markedly good agreement between experimental data and predictions was achieved.

The CCDM approach has also been applied to fluidised beds as reviewed by Rowe and Nienow (Rowe and Nienow, 1976) and Feng and Yu (Feng and Yu, 2004) and applied by Feng and Yu (Feng and Yu, 2008) to the chaotic motion of particles of different sizes in a gas fluidized bed. Kafuia et al. (Kafuia et al., 2002) describe discrete particle-continuum fluid modelling of gas-solid fluidised beds.

However, current CCDM approaches should be extended to a truly multi-phase flow behaviour as opposed to the Volume-of-Fluid method and the multi-phase mixture model (Wang, 1998). Furthermore, particle shapes other than spherical geometries have to be taken into account to meet engineering needs according to Zhu et al. (Zhu et al., 2007, 2008). This efforts should ideally be complemented by poly-disperse particle systems since all derivations have done for mono-sized particles as stated by Feng and Yu (Feng and Yu, 2004). All these efforts should contribute to a general link between continuum and discrete approaches so that results are quantified for process modelling.

In order to develop a reliable design for burners, furnaces and similar devices an accurate prediction of heat transfer rates due to radiation is required. Conductive and convective heat transfer rates depend on the temperature difference, while radiative heat transfer is proportional to the fourth power of the temperature. Thus, radiative heat transfer becomes the dominant mode at higher temperatures and may amount of up to 40% in fluidized bed combustion as estimated by Tien et al. (Tien, 1988) and 90% in large-scale coal combustion chambers as evaluated by Manickavasagam and Menguc (Manickavasagam and Menguc, 1993).

Heat transfer of fluidised beds has a large impact on performance and has been studied by different approaches (Kunii and Levenspiel, 1991; Andeen and Glicksman, 1976; Boterill, 1975; Linjewile et al., 1993). Parmar and Hayhurst (Parmar and Hayhurst, 2002) evaluated experimentally heat transfer of freely moving phosphor bronze spheres (diam. 2-8 mm) in a fluidised bed and reported improved correlations as compared to those of Ross et al. (Ross et al., 1981), Tamarin et al. (Tamarin et al., 1982), Prins (Prins, 1987) and Agarwal (Agarwal, 1991). Mickley and Fairbanks (Mickley and Fairbanks, 1955) emphasized the unsteady character of heat transfer. Collier et al. (Collier et al., 2004) derived a Nusselt number for the regime when the velocity is smaller than the minimum fluidisation velocity and found that above this regime the Nusselt number appears to be constant. The predicted results of Schmidt et al. (Schmidt and Renz, 1999; Schmidt et al., 1999; Schmidt and Renz, 2000) showed a strong dependence of heat transfer coefficients on local solid volume distribution. Similarly, Papadikis et al. (Papadikis et al., 2010) showed the heat transfer depends strongly on particle size, and thus, effects the yields of pyrolysis significantly.

Although the CCDM methodology has been established over the past decade (Tsuji et al., 1993; Xu and Yu, 1997), prediction of heat transfer is still in its infancy. Kaneko et al. (Kaneko

et al., 1999) predicted heat transfer for polymerisation reactions in gas-fluidised beds by the Ranz-Marshall correlation (Ranz and Marshall, 1952), however, excluding conduction. Swasdisevi et al. (Swasdisevi et al., 2005) predicted heat transfer in a two-dimensional spouted bed by convective transfer solely. Conduction between particles as a mode of heat transfer was considered by Li and Mason (Li and Mason, 2000, 2002; Li et al., 2003) for gas-solid transport in horizontal pipes. Zhou et al. (Zhou et al., 2004a,b) modelled coal combustion in a gas-fluidised bed including both convective and conductive heat transfer. Although, Wang et al. (Wang et al., 2011) used the two-fluid model to predict the gas-solid flow in a high-density circulating fluidized bed, Malone and Xu (Malone and Xu, 2008) predicted heat transfer in liquid-fluidised beds by the CCDM method and stressed the fact that deeper investigations into heat transfer are required.

2 Numerical Concept

This section describes the methodology of the Extended Discrete Element Method in conjunction with the numerical approaches of both continuous and discrete solvers. The latter is referred to as the Discrete Particle Method (DPM) and predicts both motion and thermodynamic state of particles.

Fortunately, a general solution approach has evolved over time, that continuous solvers for field problems follow. A set of partial differential equations, for example conservation equations for mass, momentum and energy in fluid dynamics (Hirsch, 1991; Ferzinger and Peric, 1996) and the Navier equations (Zienkiewicz, 1984; Bathe, 1996) in structural mechanics is transformed into a system of algebraic equations by discretisation that are solved on a computer. It yields results at discrete locations in time and space. Despite many approaches to discretisation, the two methods of choice and mostly applied are the Finite Volume Method (FVM) and Finite Element Method (FEM). Each of the methods may be derived from the weighted residual technique (Finlayson, 1972), and therefore, allows a generic approach to develop an interface to discrete solution methods.

Although either method is equally applicable to partial differential equations, the majority of software for Computational Fluid Dynamics is based on the Finite Volume Method, whereas the Finite Element Method is dominant in domains such as structural engineering or electro-magnetics. Hence, a generic interface to the Finite Volume Method covers software mainly developed for Computational Fluid Dynamics, whereas a coupling to the Finite Element Method includes the majority of software products dedicated to the Finite Element Analysis. Hence, by directing the focus onto numerical methods rather than particular software products, a universal and unique methodology is developed that is applicable to a variety of numerical codes. Only below this level of a generic interface the concept will branch out to a palette of software products.

Therefore, continuous solvers encompass a Finite Element solver represented by Diffpack (Langtangen, 2002) and a Computational Fluid Dynamics solver namely OpenFoam (http://www.openfoam.com, 2012). Both solvers Diffpack and OpenFoam are coupled to the Discrete Particle Method and applied to representative examples to emphasise the predictive capability of the Extended Discrete Element Method.

Other methods such as spectral methods (Canuto et al., 1987), Lattice Boltzmann (Kingdon et al., 1992) methods or cellular automata are employed to a small extent only, and therefore, are not relevant to applications in industry and are currently excluded from the analysis of this study. Spectral methods are less suited for CFD software but are important in some fields such as direct simulation of turbulence (Ferzinger and Peric, 1996). A more complete description is found in Canuto et al. (Canuto et al., 1987).

2.1 Methodology

Multi-physics problems dealt with in the proposed study include a discrete and a continuous phase, and therefore, are too complex to be solved analytically. Complementary to experiments a coupling of discrete and continuous numerical simulation methods promises a large potential for analyses. Although research and development of numerical methods in each domains of discrete and continuous solvers is still progressing, respective software tools have reached a high degree of maturity. In order to couple discrete and continuous approaches, two major concepts are available:

- **Monolithic concept:** The equations describing multi-physics phenomena are solved simultaneously by a single solver producing a complete solution.
- **Partitioned or staggered concept:** The equations describing multi-physics phenomena are solved sequentially by appropriately tailored and distinct solvers with passing the results of one analysis as a load to the next.

The former concept requires a solver that includes a combination of all physical problems involved, and therefore, requires a large implementation effort. However, there exist scenarios for which it is difficult to arrange the coefficients of combined differential equations in one matrix. A partitioned concept depicted in fig. 1 as a coupling between a number of solvers representing individual domains of physics offers distinctive advantages over a monolithic concept.

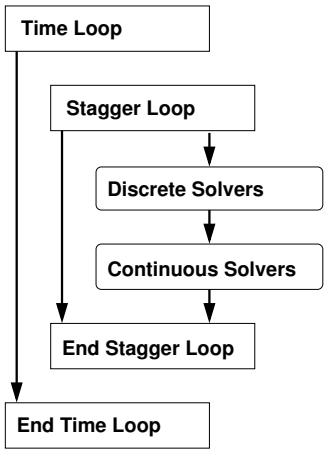

Figure 1: Staggered methodology for discrete/continuous applications

It inherently encompasses a large degree of flexibility by coupling an almost arbitrary number of solvers. However, the number of solvers usually does not exceed a number of 3 or 4 for industrial applications, also taking the CPU time requirements into account. Furthermore, a more modular software development is retained that allows by far more specific solver techniques adequate to the problems addressed.

For this purpose a generic concept with a solver module including discrete and continuous solvers independent of specific software products is to be employed that enables a coupling between discrete and continuous numerical simulation methods as shown in fig. 2.
Starting from a common CAD input the AMST solver module controls a correct transfer of scalars, vectors and tensors such as heat/mass transfer, forces or heat fluxes between the discrete and continuous solvers that produce their own results. They may be analysed commonly in a team or individually by experts of the respective disciplines.

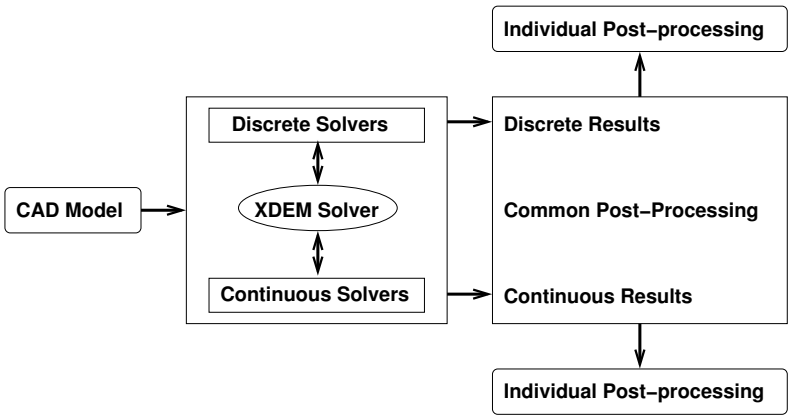

Figure 2: AMST solver module

The coupling algorithms between the Discrete Particle Method and the Finite Volume e.g. Computational Fluid Dynamics and the Finite Element Method e.g. structural engineering is dealt with by two fundamental concepts:

1. An exchange of data at the boundaries between discrete and continuous domains which represents at the point of contact a transfer of forces or fluxes such as heat or electrical charge
2. An exchange of data from particles submerged in the continuous phases into the continuous domain by volumetric sources

The former defines additional boundary conditions for the continuous phase, while the latter coupling appears as source terms in the relevant partial differential equations. Hence, applying appropriate boundary conditions and volumetric sources for the discrete and continuous domain furnishes a consistent and effective coupling mechanism.

2.2 Computational Fluid Dynamics Solver: OpenFoam

The Finite Volume Method (Patankar, 1980; Ferzinger and Peric, 1996; Blevins, 1984) requires the computational domain to be subdivided into a finite number of contiguous control volumes to which are the integral forms of the conservation equations are applied. Surface and volume integrals are approximated by quadrature formulas that yield a system of algebraic equations. Its solution furnishes the values of the variables at the centroids of the control volumes. Since conservation principles are fulfilled for each control volume, the method is conservative over the entire simulation domain. The method can handle any type grid, and therefore, can accommodate complex geometries.

2.3 Finite Element Solver: Diffpack

Similar to the Finite Volume Method, the Finite Element Method (Taylor and Hughes, 1981; Zienkiewicz, 1984; Bathe, 1996) requires the solution domain to be subdivided into discrete volumes also referred to as finite elements. Hence, the method is also suited to complex geometries. Within the finite elements shape functions are defined, that approximate the solution in each element. This approximation is substituted into the weighed volume integral leading to an algebraic system, of which the solution approximates the distribution.

2.4 Discrete Particle Method

Granular materials play a very important role in engineering technology and according to Richard "Granular materials are ubiquitous in nature and are the second-most manipulated material in industry (the first one is water)" (Richard, 2005). Hence, granular materials are commercially important in applications as diverse as agriculture, pharmaceutical and food industry, and energy production. Some predominant examples are rice, coffee, corn flakes, nuts, coal, sand, fertilizer and ball bearings. Due to its size a powder is a special case and is more cohesive and more easily fluidised in a gas. Therefore, research into granular materials is a challenging and directly applicable task in engineering.

Contrary to continuum mechanics the microscopic length scale i.e. size of the grains is comparable to the geometric dimensions. Therefore, an approach is required that tracks each entity of a granular material individually. The constituents of granular material must be sufficiently large, so that they do not undergo thermal motion fluctuations. Thus, the lower length scale for a granular material is $\sim 1.0\mu m$, whereas the upper size limit may extend as large ice floes or asteroid belts of solar systems.

The Discrete Particle Method is derived from the classical Discrete Element Method (DEM) (Cundall and Strack, 1979; Pöschel and Schwager, 2005; Allen and Tildesley, 1990; Landau and Lifshitz, 1960; Sadus, 1999; Crowe et al., 1998; Bridgewater, 1994; Duran and Gennes, 1999) to arrive at the Extended Discrete Element Method. It enriches the classical method by predicting the thermodynamic state of particles and by a variety of interfaces to continuous solvers such as fluid dynamics and stress/strain analysis, and thus, helps alleviate the shortcomings of the Discrete Element Method that does not provide results on the thermodynamic state of particles. The motion module of the Discrete Particle Method handles a sufficient number of geometric shapes that are believed to cover a large range of engineering applications, while the thermodynamics module incorporates a physical-chemical approach that describes temperature and arbitrary reaction processes for each particle in an ensemble. Relevant areas of application include furnaces for wood combustion, blast furnaces for steel production, fluidised beds, cement industry or predictions of emissions from combustion of coal or biomass.

The Discrete Particle Method (DPM) considers each particle of an ensemble as an individual entity with motion and thermodynamics properties. The motion module of the DPM can handle numerous geometric shapes that are believed to cover a large range of engineering applications. The thermodynamics module incorporates a physical-chemical approach that describes the temperature and arbitrary reaction processes for each particle in an ensemble.

This concept offers a large degree of detail on both motion and conversion that serves to deepen and expand knowledge for a wide range of engineering applications. Each of these applications represents complex processes involving various aspects of thermodynamics, chemistry and physics. Hence, the Extended Discrete Particle Method as an advanced multi-physics and numerical simulation tool that deals with both motion and chemical conversion of particulate material. However, predictions of solely motion or conversion in a decoupled mode are also applicable.

2.4.1 Conversion Module

A discrete particle is considered to consist of a gas, liquid, solid and inert phase whereby local thermal equilibrium between the phases is assumed. It is based on the assessment of the ratio of heat transfer by conduction to the rate of heat transfer by convection expressed by the Peclet number as described by Peters (Peters, 1999) and Kansa et al. (Kansa et al., 1977). The gas phase represents the porous structure e.g. porosity of a particle and is assumed to behave as an ideal gas. According to Man and Byeong (Man and Byeong, 1994) one-dimensional differential conservation equations for mass, momentum and energy are sufficiently accurate. Transport by diffusion has to

be augmented by convection as stated by Rattea et al. (Rattea et al., 2009) and Chan et al. (Chan et al., 1985). In general, the inertial terms of the momentum equation is negligible due to a small pore diameter and a low Reynolds number (Kansa et al., 1977). However, for generality, the inertial terms may be taken into account by the current formulation. The importance of a transient behaviour is stressed by Lee et al. (Lee et al., 1995, 1996).

Each of the phases may undergo various conversion based on both homogeneous and heterogeneous reactions whereby the products may experience a phase change such as encountered during drying i.e. evaporation. The need for more elaborate models of heterogeneous reactions was pointed out by Chapman (Chapman, June 5 - 7, 1996). In addition, intrinsic rate modelling is applied to the current model to capture accurately the nature of various reaction process as pointed out by Rogers et al. (Rogers et al., 1975) and Hellwig (Hellwig, 1988). Furthermore, morphological changes in conjunction with a regressing size are accounted for.

Thus, the Discrete Particle Model (DPM) offers a high level of detailed information and, therefore, is assumed to omit empirical correlations, which makes it independent of particular experimental conditions for both a single particle and a packed bed of particles. Such a model covers a larger spectrum of validity than an integral approach and considerably contributes to the detailed understanding of the process (Specht, 1993; Laurendeau, 1978; Essenhigh et al., 1999). Hence, process of thermal conversion is described by a set of one-dimensional and transient differential conservation equations applied to the solid, liquid and gaseous phase, whereby the solid and liquid species are considered as immobile. The predictions include major properties such as temperature and species distribution inside a particle. Thus, a description by conservation equations does not bound the reactions to a finite temperature range, so that they take place simultaneously, or to a reaction mode, such as a reacting- or a shrinking-core mode. In detail, the following assumptions are made to describe conversion of a particle

- a particle consists of a solid and a gaseous porous phase that may be accompanied by a liquid phase
- thermal equilibrium between gaseous, liquid and solid phases inside a particle
- particle geometry represented by slab, cylinder or sphere
- description by one-dimensional and transient differential conservation equations for mass, momentum and energy
- convective and diffusive transport in the gas phase through Darcy flow
- average transport properties for diffusion and conduction inside a particle
- thermal conversion described by homogeneous, heterogeneous and intrinsic rate modelling
- evolution of morphological parameters i.e. porosity and inner surface
- regressing surface of a particle during mainly combustion and gasification processes

Conservation of Mass

Conservation of mass for the porous gas phase writes as follows:

$$\epsilon \frac{\partial \rho_g}{\partial t} + \frac{1}{r^n} \frac{\partial}{\partial r} \left(r^n \rho_g \vec{v}_g \right) = S_{mass} \tag{1}$$

where ϵ, ρ $\vec{v}$ and S_{mass} denote porosity of the particle, gas density, velocity and mass sources due to a transfer between the solid/liquid phase to the gas phase and its reactions, respectively.

Due to a general formulation of the conservation equation with the independent variable r as a characteristic dimension the geometrical domain can be considered an infinite plate ($n = 0$), an infinite cylinder ($n = 1$) or a sphere ($n = 2$).

Conservation of Momentum

Transport of gaseous species within the porous space of a particle is approximated by a Darcy flow. An analysis of orders of the relevant terms yields (Blevins, 1984), that convective terms are negligible and consequently the effect of friction is described by the Darcy and Forchheiner correlation. Hence, the following balance of linear momentum is applied:

$$\epsilon \frac{\partial \rho_g \vec{v}_g}{\partial t} = -\frac{\partial p}{\partial r} - \frac{\mu}{k}\vec{v}_g - C\rho_g \vec{v}_g \mid \vec{v}_g \mid \tag{2}$$

where p, μ, k and C stand for pressure, viscosity, permeability and Forchheimer coefficient, respectively. In general, the inertial terms may be neglected, however, are kept within the present formulation. The solution of the continuity and momentum equation furnishes a gas velocity within the porous part of the particle.

Conservation of Species

Convection in conjunction with diffuse transport describes the distribution of gaseous species i in the porous particle versus time and space as follows:

$$\frac{\partial \rho_{i,g}}{\partial t} + \frac{1}{r^n}\frac{\partial}{\partial r}\left(r^n \vec{v}_g\, \rho_{i,g}\right) = \frac{1}{r^n}\frac{\partial}{\partial r}\left(r^n \frac{D_{i,eff}}{M_i}\frac{\partial \rho_{i,g}}{\partial r}\right) + \sum_{k=1}^{l} \dot{\omega}_{k,i} \tag{3}$$

where $\rho_{i,g}$ and $\dot{\omega}_{k,i}$ are partial density of gaseous specie i and a reaction source. As a result of the averaging process and the influence of tortuosity τ on the diffusion, an effective diffusion coefficient is derived as follows (Shih-I, 1977; Dullien, 1979):

$$D_{i,eff} = D_i \frac{\epsilon_P}{\tau} \tag{4}$$

where ϵ_P is the porosity of the particle and the molecular diffusion coefficients D_i are taken from the equivalent ones of the appropriate species in nitrogen.

Similaraly, conservation for both liquid and solid species writes as follows

$$\frac{\partial \rho_{i,liquid}}{\partial t} = \sum_{k=1}^{l} \dot{\omega}_{k,i,liquid} \tag{5}$$

$$\frac{\partial \rho_{i,solid}}{\partial t} = \sum_{k=1}^{l} \dot{\omega}_{k,i,solid} \tag{6}$$

where the right hand side comprises all reactions k involving a specie i, each of which is characterised by specific kinetic parameters (Aho, 1987; Saastamoinen et al., 1993; J. J. Saastamoinen and J.-R.; Saastamoinen and Richard, 1998). Due to intrinsic rate modelling of the current approach, reaction regimes (Peters, 1999) of a shrinking- and a reacting-core mode are distinguished. Depending on the rate-limiting process, the depletion of solid material therefore results in either a decreasing particle density or a reduction of particle size (Peters, 1999, July 14 - 17, 1997). The latter causes a decreasing height of a reacting bed.

The distribution of porosity ϵ and specific inner surface S are determined by the following equations

$$\frac{\partial \epsilon}{\partial t} = \frac{M_\mathrm{s}}{\rho_\mathrm{s}\delta}\,\dot{\omega}_\mathrm{s} \tag{7}$$

$$\frac{\partial S}{\partial t} = \frac{1-\epsilon^\mathrm{o}}{c_\mathrm{s}^\mathrm{o}}\,\dot{\omega}_\mathrm{s} \tag{8}$$

where M_s, c_s, $\dot{\omega}_\mathrm{s}$ and δ denote the molecular weight, concentration of solid material, reaction rate of solid material and characteristic pore length, respectively (Peters, July 14 - 17, 1997; Peters and Bruch, 2001). The superscript "o" stands for initial values of the appropriate variable.

Conservation of Energy

Due to a negligible heat capacity of the gas phase compared to the liquid and solid phase conservation of energy includes solids and liquids only (local thermal equilibrium):

$$\frac{\partial\left(\sum_{i=1}^{k}\rho_i c_{p,i} T\right)}{\partial t} = \frac{1}{r^n}\frac{\partial}{\partial r}\left(r^n \lambda_{eff}\frac{\partial T}{\partial r}\right) + \sum_{k=1}^{l}\dot{\omega}_k H_k \tag{9}$$

The locally varying conductivity λ_{eff} is evalauted as (Gronli, 1996)

$$\lambda_{eff} = \epsilon_P \lambda_g + \sum_{i=1}^{k}\eta_i \lambda_{i,solid} + \lambda_{rad} \tag{10}$$

which takes into account heat transfer by conduction in the gas, solid, char and radiation in the pore. The latter is approximated as

$$\lambda_{rad} = \frac{\epsilon}{1-\epsilon}\,\sigma\, 4.0\, T^3 \tag{11}$$

where ϵ, σ and T stand for porosity, Boltzmann constant and temperature, respectively. The source term on the right hand side represents heat release or consumption due to chemical reactions.

Initial and Boundary Conditions

In order to complete the mathematical formulation of the problem, initial and boundary conditions must be provided. A wide range of experimental work has already been carried out in this field and appropriate laws in terms of Nusselt and Sherwood numbers are well established for different geometries and flow conditions. Good compilations can be found in (Specht, 1993; Bird et al., 1960; Botterill, 1975; Bejan, 1984; Grigull, 1963; Brauer, 1971). The following boundary conditions for mass and heat transfer of a particle are applied:

$$-\lambda_{eff}\frac{\partial T}{\partial r}\,|_R = \alpha(T_R - T_\infty) + \dot{q}_{rad} + \dot{q}_{cond} \tag{12}$$

$$-D_{i,\mathrm{eff}}\frac{\partial c_i}{\partial r}\,|_R = \beta_i(c_{i,R} - c_{i,\infty}) \tag{13}$$

where T_∞, $c_{i,\infty}$, α and β denote ambient gas temperature, concentration of specie i, heat and mass transfer coefficients, respectively. The mass transfer coefficients employed are valid for vanishing

convective fluxes. In the case convective fluxes e.g. volatiles and vapour out of and into the particle are important transfer coefficients have to be corrected according to the Stefan correction as follows (Bird et al., 1960):

$$\alpha = \frac{\dot{m}_g \, c_{p,g}}{\exp(\dot{m}_g \, c_{p,g}/\alpha_0) - 1} \tag{14}$$

$$\beta = \frac{\dot{m}_g/\rho_g}{\exp(\dot{m}_g/\rho_g \, \beta_0) - 1} \tag{15}$$

where α_0 and β_0 denote the transfer coefficients for a vanishing convective flux over the particle surface. These coefficients are larger than those of the film theory for a convective flow out of the particle and smaller for a flow directed into the particle.

2.4.2 Motion Module

As above-mentioned an ensemble of discrete and moving particles offers the highest potential to describe transport processes. Each of the particles is assumed to have different shapes, sizes and mechanical properties. Shapes such as barrel, block, cone, cube, cylinder, disc, double-cone, ellipsoid, hyperboloid , parallel-epiped, sphere, tetrahedron, torus, wall and pipe are available.

Thus, the motion of particles is characterised by the motion of a rigid body through six degrees of freedom for translation along the three directions in space and rotation about the centre-of-mass as depicted in fig. 3.

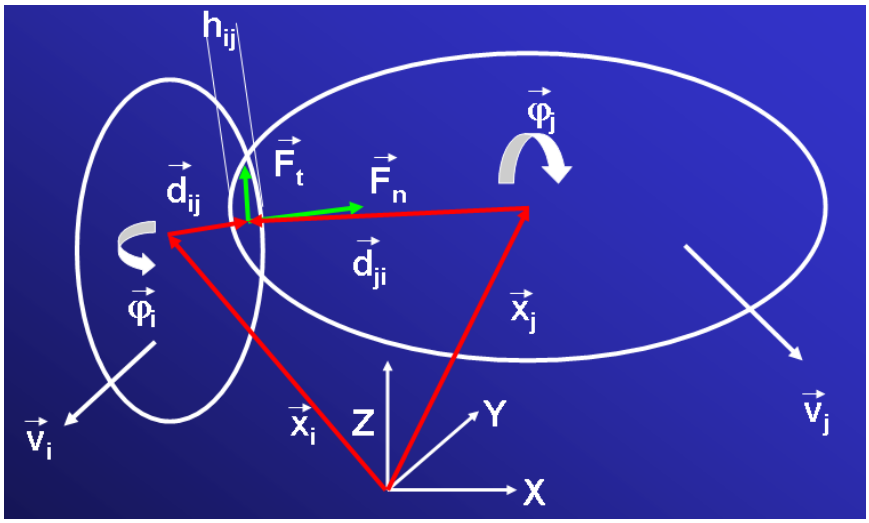

Figure 3: Particles in contact

By describing these degrees of freedom for each particle its motion is entirely determined. Newton's Second Law for conservation of linear and angular momentum describe position and orientation of a particle i as follows:

$$m_i \frac{d^2\vec{r}_i}{dt^2} = \sum_{i=1}^{N} \vec{F}_{ij}(\vec{r}_j, \vec{v}_j, \vec{\phi}_j, \vec{\omega}_j) + \vec{F}_{extern} \tag{16}$$

$$\bar{I}_i \frac{d^2\vec{\phi}_i}{dt^2} = \sum_{i=1}^{N} \vec{M}_{ij}(\vec{r}_j, \vec{v}_j, \vec{\phi}_j, \vec{\omega}_j) + \vec{M}_{extern} \tag{17}$$

where $\vec{F}_{ij}(\vec{r}_j, \vec{v}_j, \vec{\phi}_j, \vec{\omega}_j)$ and $\vec{M}_{ij}(\vec{r}_j, \vec{v}_j, \vec{\phi}_j, \vec{\omega}_j)$ are the forces and torquues acting on a particle i of mass m_i and tensor moment of inertia $\bar{I}_i$. Both forces and torques depend on position $\vec{r}_j$, velocity $\vec{v}_j$, orientation $\vec{\phi}_j$, and angular velocity $\vec{\omega}_j$ of neighbour particles j that undergo impact with particle i. The contact forces comprise all forces as a result from material contacts between a particle and its neighbours. Forces may include external forces due to moving grate bars, fluid forces and contact forces between the particles in contact with a bounding wall. This results in a system of coupled non-linear differential equations which usually cannot be solved analytically.

The Discrete Element Method (DEM), also called a Distinct Element Method, is probably the most often applied numerical approach to describe the trajectories of all particles in a system. Thus, DEM is a widely accepted and effective method to address engineering problems in granular and discontinuous materials, especially in granular flows, rock mechanics, and powder mechanics. Pioneering work in this domain has been carried out by Cundall (Cundall and Strack, 1979), Haff (Haff and Werner, 1986), Herrmann (Gallas et al., 1992) and Walton (Walton and Braun, 1986). The volume of Allen and Tildesley (Allen and Tildesley, 1990) is perceived as a standard reference for this field. For a more detailed review the reader is referred to Peters (Peters and Džiugys, 2001).

As above-mentioned particles of a granular media exert forces on each other only during mechanical contact. Once the particles are in contact the repulsive force increases with a sharp gradient due to the rigidity of the particles. Therefore, a rather small time step has to be chosen to resolve the impact between particles accurately.

Therefore, in a computational approach, the deformation of two particles in contact may be approximated by a representative overlap h (Cundall and Strack, 1979) as depicted in fig. 4.

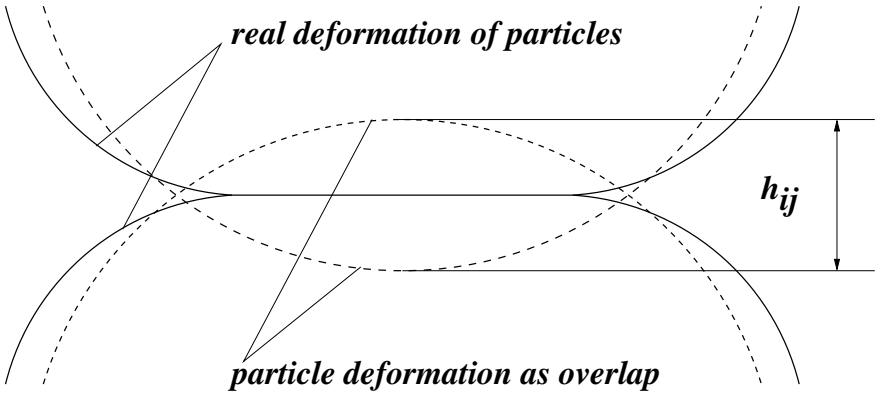

Figure 4: Approximation of particle deformation during impact through a respective overlap area

The resulting force $\vec{F}_{ij}$ due to contact may be decomposed into its normal and tangential components

$$\vec{F}_{ij} = \vec{F}_{n,ij} + \vec{F}_{t,ij} \tag{18}$$

where the components additionally depend on displacements and velocities normal and tangential to the point of impact between the particles. In a simple approach the analogy to a spring for an ideal elastic impact serves to determine the contact force as $\vec{F}_{ij} = k_{ij}\vec{h}_{ij}$. However, for more sophisticated applications additional influences such as non-linearity, dissipation or hysteresis need to be taken into account. For a detailed discussion of inter-particle forces the reader is referred to Peters (Peters, 2003; Pöschel and Schwager, 2005)

3 Relevant Engineering Applications

Multi-physics analysis can be applied to numerous engineering applications that involve the coupling of multiple physical phenomena of particulate/granular materials. Both continuous and discrete results reveal a large degree of details that contribute to a better understanding of the under-lying physics, and thus, help to improve design and operating conditions. Out of the numerous applications are those selected that are believed to highlight particular potentials of the presented method and that distinguish it from classical approaches. Among the applications chosen are examples from reaction engineering e.g. packed and moving bed reactors and particle-structure interaction. Due to the large amount of detailed results obtained by the current method, in general only those are presented that emphasise the the extended predictive capabilities of the method and results emanating from the classical DEM or CFD approach are largely omitted because they do not present any novel features.

Fluid-structure interaction (FSI) refers to a coupling between two continuous media which is outside the scope of this contribution. For a further details on FSI, the reader is referred to Langtangen (Langtangen, 2002).

3.1 Thermal Conversion in a Packed Bed Reactor

Packed bed reactors dominate a broad range of engineering applications of which a blast furnace is a pre-dominant example. Common to all these devices is heat transfer between the solid particles and the gas flow streaming through the void space between the particles. Hence, the gas phase is coupled to the particle surfaces by heat transfer. For a classical continuous representation of the particulate phase either experimental data or empirical correlations have to be employed that determine both total surface of the particles and the distribution of void space between them. However, these disadvantages are alleviated by the current approach that allows evaluating both available surface for heat transfer and void space affecting the flow distribution. Both particle surface and void space are determined by filling a reactor vessel with bi-disperse particles of which the final arrangement of particles has been predicted and is shown in fig. 5.

For a spherical particle or any other given geometry of a particle its surface is known to determine heat transfer conditions. In addition, the position of each particle in a packed bed as shown in fig. 5 is determined so that the predicted conditions of the gas flow in the vicinity of the particle are identifiable to assess local heat transfer. Among these parameters influencing heat transfer significantly is the local velocity e.g. distribution of flow in the void space of the packed bed that depends on the distribution of the void space i.e. porosity in a packed bed to a large extend. With known position and size of particles the porosity distribution is readily determined of which two cross-sectional distributions for the larger and smaller spheres is shown in the following fig. 6.

Fig. 6 highlights two obvious characteristics of packed beds: Different levels of porosity for arrangements of differently sized spherical particles and the so-called wall effect. The latter is manifested by an increased porosity in the vicinity of the inner walls reaching values of porosity of ~ 0.5 at corners in particular. In these regions the gas flow experiences less drag that results in higher flow velocities past the walls. It contributes to an increased heat transfer to the walls as

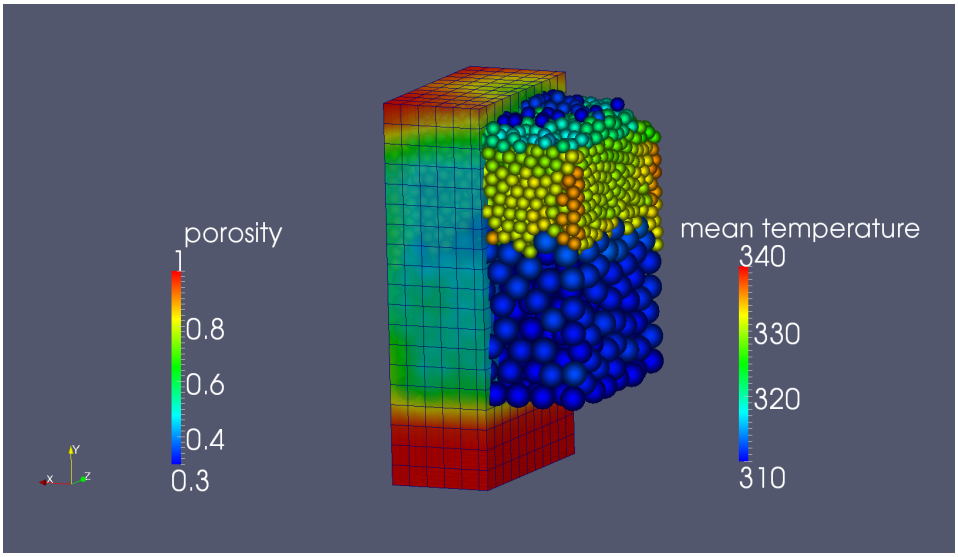

Figure 5: Predicted arrangement of particles in a packed bed reactor

depicted in fig. 5, and thus causes higher thermal losses of the entire reactor. Since both porosity and flow velocity near the walls are predicted accurately, heat losses for packed bed reactors may be determined without further experiments or near wall correlations.

Furthermore, different levels of porosity are evaluated in the bulk for smaller and larger sized particles as shown in fig. 6a and 6b. An arrangement of smaller particles usually yields lower levels of porosity than found for larger particles positioned in a packed bed. Thus, the bulk porosities for the arrangement of large and small particles in fig. 6a and 6b amounts to ~ 0.4 and ~ 0.34, respectively. Similarly, the vertical velocity component of the bulk flow is affected by the porosity distribution in the lower and upper part of the packed bed. Since larger void space is available for the flow in the lower part of the packed bed, lower velocities are observed whereas the bulk velocity in the upper part of the reactor has to increase due to a reduced porosity. Furthermore, the gas velocity is significantly increased by ~ 50 % as compared to the bulk velocity due to higher porosity near the walls and the corners in particular.

The convective heat transfer above-mentioned is defined through Nusselt numbers. Heat transfer and also mass transfer rates are augmented by the tortuosity of the flow paths as compared to a single particle (Baehr and Stephan, 1994). According to Schlünder and Tsotsas (Schlünder and Tsotsas, 1988) the appropriate Nusselt number $\mathrm{Nu_B}$ and Sherwood number Sh_B for a packed bed are derived from those a single particle $\mathrm{Nu_P}$ and Sh_P by the following relation:

$$\mathrm{Nu_B} = f\,\mathrm{Nu_P} \tag{19}$$

$$\mathrm{Sh_B} = f\,\mathrm{Sh_P} \tag{20}$$

The correlation coefficient f is determined by the following relationship (Gnielinski, 1982):

$$f = 1 + 1.5\,(1 - \epsilon_P), \tag{21}$$

with ϵ_P denoting the void fraction of the packed bed.

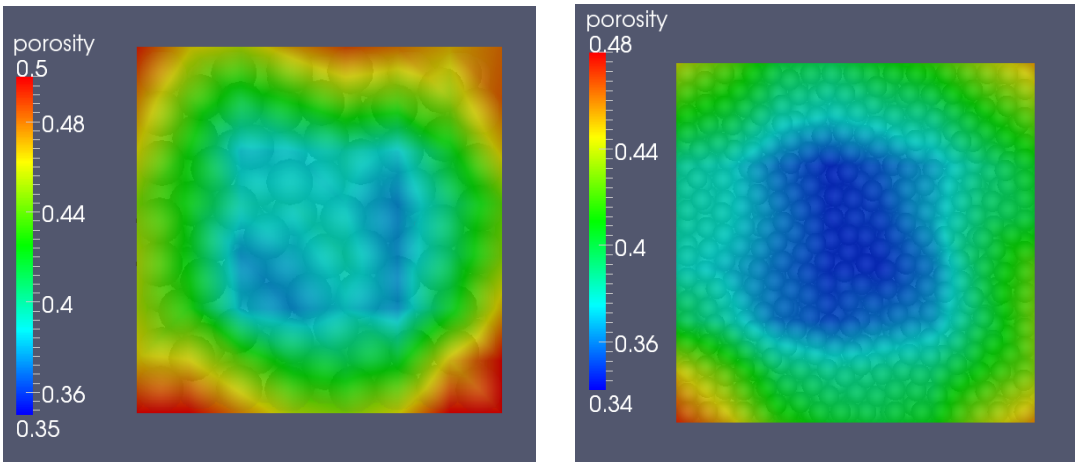

(a) Distribution of porosity in an arrangement of large spheres (D = 0.1 m)

(b) Distribution of porosity in an arrangement of small spheres (D = 0.05 m)

Figure 6: Distribution of porosity in two cross-sectional areas in the upper and lower part of a packed bed reactor

In addition to heat transfer to the gas phase, further transfer occurs between particles in physical contact through conduction. The conductive heat flux $\dot{q}_{cond}$ referred to in eq. 12 between two neighbouring particles in contact is estimated by

$$\begin{aligned} \dot{q}_{\text{cond}} &= -\frac{1}{1/\lambda_1 + 1/\lambda_2}\frac{\partial T}{\partial r}, \\ &\approx -\frac{1}{1/\lambda_1 + 1/\lambda_2}\frac{T_{\text{S},1} - T_{\text{S},2}}{\Delta r_{\text{S},1} - \Delta r_{\text{S},2}} \end{aligned} \tag{22}$$

where the temperature gradient between two particles is approximated by the temperature difference between the outer shell values of the particles and the distance $\Delta r_{\text{S,i}}$ from the outer particle surface. The conductivities λ_1 and λ_2 refer to the particles in contact, respectively. The contact area is assumed to be quadratic and determined by the contact angles γ_1 and γ_2, as sketched in fig. 8.

$$A_c = \frac{1}{2}((R_1 \tan\gamma_1)^2 + (R_2 \tan\gamma_2)^2). \tag{23}$$

At higher temperatures, a particle i emits a radiative flux with its surface temperature T_S and adsorbs a flux $\dot{q}_{rad,j}$ from all neighbouring particles j weighted by the respective view factor $F_{i\to j}$. Thus, the total flux due to radiation referred to by eq. 12 is given by

$$\dot{q}_{rad} = \sum_{j=1}^{K} F_{i\to j}\,\alpha\,\dot{q}_{rad,j} - \epsilon\,\sigma\,T_S^4, \tag{24}$$

where α and ϵ denote the adsorption and the emission coefficient, respectively. The view factor is determined as the ratio of the surface of particle i to the sum of the surfaces of all neighbouring particles j with

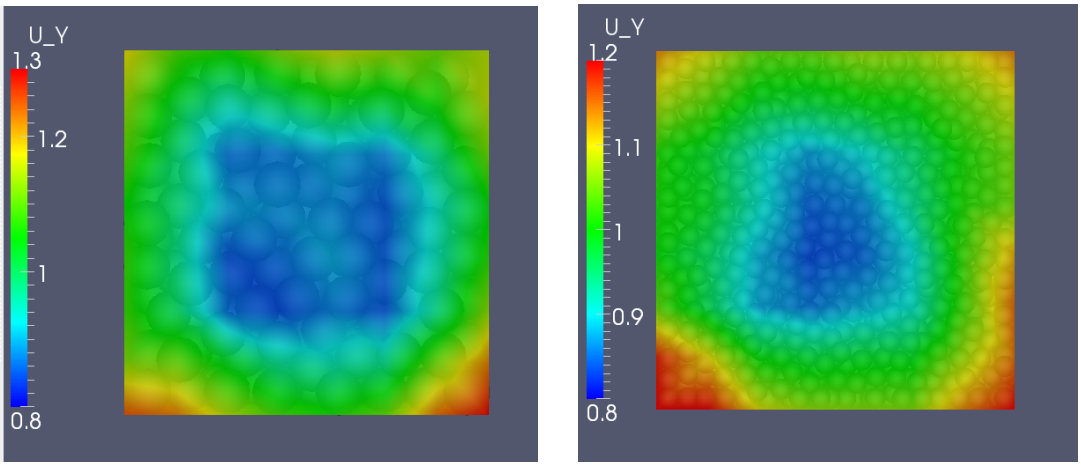

(a) Distribution of the vertical velocity component in an arrangement of large spheres (D = 0.1 m)

(b) Distribution of the vertical velocity component in an arrangement of small spheres (D = 0.05 m)

Figure 7: Distribution of the vertical velocity component in two cross-sectional areas in the upper and lower part of a packed bed reactor

$$F_{i \to j} = \frac{A_i}{\sum_j A_j}. \tag{25}$$

Pyrolysis experiments for beech wood were carried out with the PANTHA test facility (Schröder, 1999). It is a small-scale packed bed reactor as shown in fig. 5 that was filled with beechwood particles of which relevant properties are taken from Kansa et al. (Kansa, 1972) and are listed in table 1.

Particle radius R (mm)	6.2
Density ρ (kg/m^3)	750
Porosity ϵ	0.64
Permeability k (m^2)	0.02
Pore diameter (m)	$50.0 \cdot 10^{-6}$
Tortuosity	1.0
Specific Heat c_p (J/kgK)	2551.3
Conductivity λ (W/mK)	0.1256

Table 1: Beech wood properties

The temperature of the incoming gas flow varied between $T = 210°\ C$ and $T = 530°\ C$. In order to predict the mass loss of the wooden sample due to pyroylsis, three different models were used and its results were compared to experimental data. Two models belong to the class of one-step models of Kung et al. (Kung, 1972) and Balci et al. (Balci et al., 1993), whereas the remaining approach of Grønli (Gronli, 1996) consists of primary reactions with char, tar and gas as products and secondary reactions, which converts tar into gas composed of carbon monoxide and carbon dioxide. The relevant kinetic data is listed in table 2.

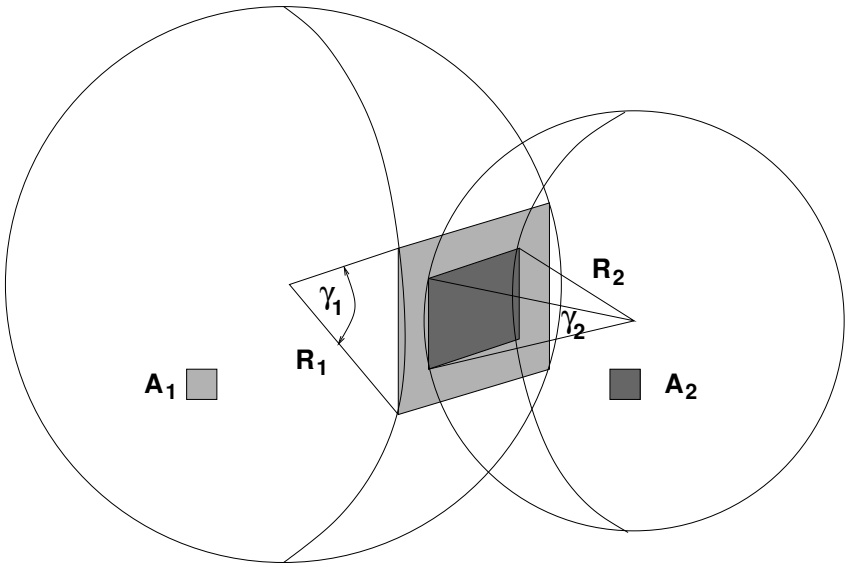

Figure 8: Contact area between two particles for heat conduction

		E_a $[kJ/mol]$	A $[1/s]$	Δh $[kJ/kg]$
Kung et al.	$k_{G,1}$	125.6	5.25 10^7	418
Balci et al.	$k_{G,1}$	123.1	1.35 10^9	-4500
Grønli	$k_{G,1}$	140	1.3 10^8	150
	$k_{T,1}$	133	2.0 10^8	150
	$k_{C,1}$	121	1.08 10^7	150
	$k_{G,2}$	80	2.3 10^4	-50

Table 2: Kinetic data for pyrolysis

The following fig. 9 depicts the comparison between measurements and predictions obtained by the above-mentioned models for a temperatures of $T = 500.0^o\ C$.

Fig. 9 shows satisfactory agreement between measurements and the pyrolysis models for an experiment carried out at a temperature of $T = 530^\circ\ C$. The best predictions were obtained by the one-step model of Balci and the three step model of Grønli, whereas the model of Kung tends to under-predict the pyrolysis rate during the period between $t = 2000$ and $t = 3000\ s$. For times $t > 3000\ s$ the final stage of pyrolysis is predicted well for these models.

3.2 Moving Bed on a Forward Acting Grate

Similar to the previous section, in which the the effects of a packed bed of two differently sized spherical particles on porosity and flow distribution was emphasised, the current section highlights the predictive capabilities of the Extended Discrete Particle Method for combustion of a moving bed of fir-wood on a forward acting grate. It differs in so far from the previous application of a steady-state packed bed reactor that particles are transported through the reaction chamber, and thus, change frequently their position within the bed. It effects also the distribution of the void space i.e. porosity that varies as function of space and time. The dynamics of particles are

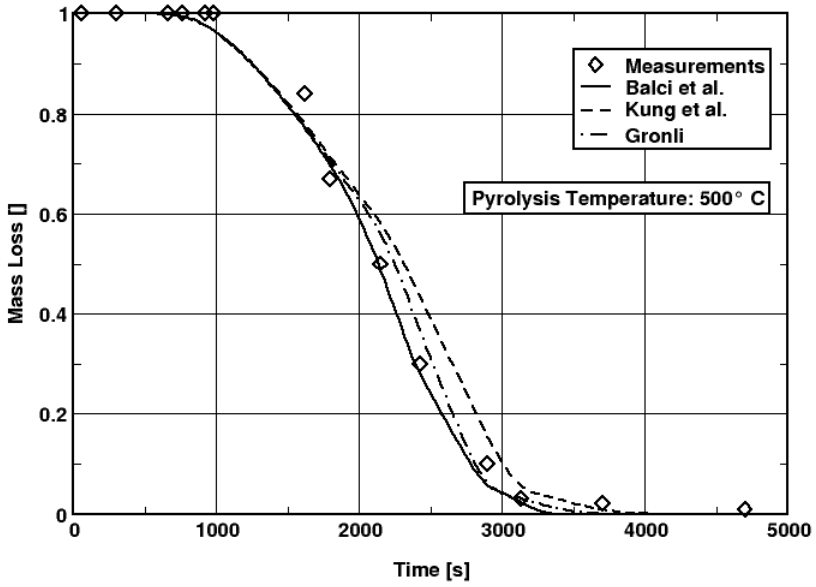

Figure 9: Pyrolysis of a packed bed of beechwood particles

predicted by the motion module of the Discrete Particle Method, whereas heat-up and conversion is determined by the thermodynamic module similar to the previous section. With the known position of each particle at any predicted incident of time, the time-dependent distribution of porosity is evaluated that influences the distribution of flow in the moving bed as a medium with temporal and spatially varying porosity. The latter is readily predicted by the current approach and does not require any experimental data or empirical correlation that are almost impossible to derive for a chaotic-like motion on a forward acting grate. Furthermore, the individually predicted motion and thermodynamic state of all particles of the moving bed provides degree of details that is not achieved by pure continuous approaches. Hence, results obtained allow a detailed analysis of the processes involved and reveal the underlying physics.

This is exemplified for a single particle of the ensemble of a moving bed in fig. 10 that depicts the evolution of the spatial distribution of temperature over a period of $\Delta t = 1000\ s$.

The particle's initial temperature was set to $T = 300.0\ K$, so that during an initial period heat is lost to the primary air causing the particle temperature to decrease. A sharp increase in temperature is recognised after a period of $\sim 100.0\ s$, because the particle was moved to the surface of the packed bed, and therefore, is exposed to a radiative flux from the furnace walls. After residing for some time at the surface of the moving bed, it enters the interior of the moving bed due to bar motion. Hence, the particle is shielded by newly evolving surface particles, and therefore, does not receive a further radiation flux. Instead it exchanges heat with particles in its proximity and due to convection, and thus, reduces its temperature. At a later stage the particle appears on the bed surface again and receives a radiative heat flux and the cycle of heating up and cooling down repeats itself irregularly during the total residence on the grate.

The moving bed itself was exposed to a constant radiative flux on its surface. A periodic

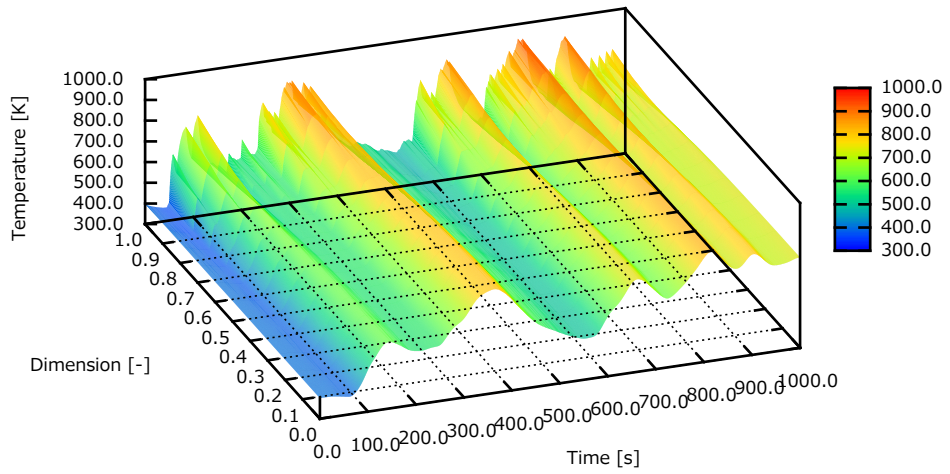

Figure 10: Temperature distribution of a particles on a backward acting grate versus time and space

forward and backward motion was applied to every second grate bar, so that bars between the moving bars were kept at rest. These kinetics representing the operation mode of a forward acting grate cause the particles to move over the grate through the combustion chamber. The predicted results are shown in fig. 11 to 13 for distribution of temperature, moisture content, and char mass fraction of the particles, respectively, at a time of t = 250 s as a representative snapshot from the entire transient results.

Although, a temperature distribution with a layered characteristic develops during heat-up of the moving bed, mixing of particles in vertical directions breaks up a strongly layered distribution. Thus, a varying amount of heat is transferred between particles. Furthermore, surface particles on top of the packed bed interchange frequently their positions with particles from the interior of the packed bed. Hence, particles are almost randomly exposed to surface radiation for a certain period and contribute to an inhomogeneous temperature distribution of the moving bed. This characteristics are also reflected by the distribution of moisture for individual particles depicted in fig. 12. Although most of the particles have been dried, there exist still particles that remain with their initial water content of 60 % located in the lower part of the packed bed, though. These findings confirm experience that drying requires a significant grate length e.g. time until all the particles are dry.

After the drying process is completed, pyrolysis follows at elevated temperatures, at which the wood matrix is converted to char. The degree of thermal degradation during pyrolysis is shown in fig. 13 indicating a rather inhomogeneous distribution of pyrolysis progress.

The latter is caused by an inhomogeneous temperature distribution due to mixing on the forward acting grate and augmented by an equally in-homogeneously distributed drying process, which delays pyrolysis. Thus, contrary to an often made assumption that a reaction front propagates from top to bottom of the packed as reported by Shin and Choi (Shin and Choi, 2000), the current approach of the Extended Discrete Element Method predicts accurate spatially distributed reaction rates. Although clusters of pyrolysed particles exist, a clearly layered reaction progress is not visible. It is supported by the discrete resolution of the particulate phase in conjunction with

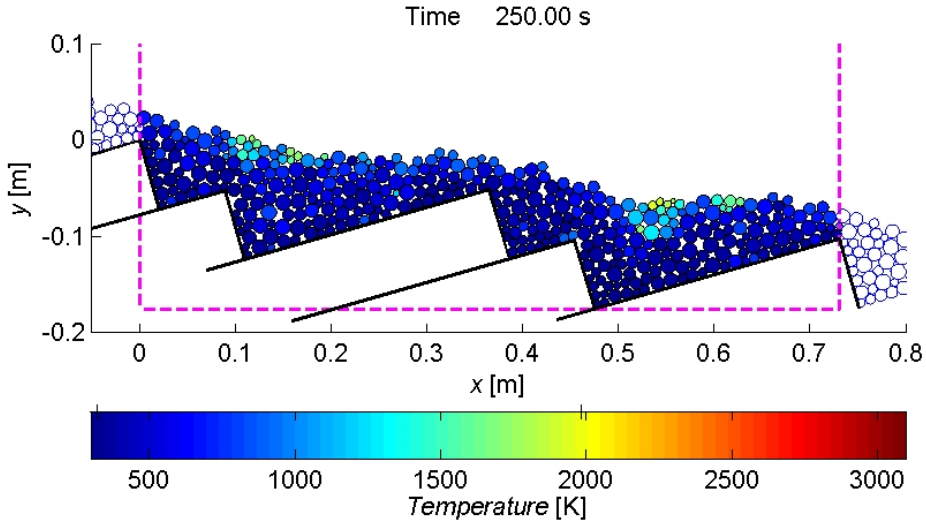

Figure 11: Temperature distribution of individual particles in a moving bed at a time of 250 s

local properties of the flow.

3.3 Fluidised Bed Reactor

The previous examples involved heat and mass transfer between the particles and the flow whereby drag forces e.g. transfer of momentum was negligible. However, a fluidised bed relies on on drag forces exerted by the fluid on the particles, and therefore, is addressed in this section, however, omitting predictions of thermodynamic states as this was already elaborated in the previous sections. Depending on the flow conditions, these drag forces of each particle vary in space and time and is taken into account by a drag loss coefficient of the following form

$$F_{drag} = c_D \, A_D \, \frac{1}{2} \rho_g \, v_r^2 \tag{26}$$

where c_D, A_D, ρ_g and v_r denote drag coefficient, surface relevant for drag, gas density and velocity of the particle relative to the gas flow, respectively.

The drag force acts as an external force on a particle referred to in eq. 16 and enters conservation of momentum as a volumetric loss term, and thus, completes the coupling between solid and gas phase. In addition to drag forces, forces resulting from inter-particle collisions were taken into account and were modelled by Hooke's law. Relevant properties of the particles are given in the following table 3:

Particles were fluidised in a conical reactor through which a gas at ambient conditions with a velocity of $v = 30 \; m/s$ entered. Due to an expansion of the reactor into the flow direction, velocities reduce, so that fluidisation takes place over a certain region. The extension of this region is dependent on the turbulent fluctuations, which cause an instantaneous fluctuation of the drag force as discussed by Eaton (Eaton, 2009), Crowe (Crowe, 2000) and Nasr and Ahmadi (Nasr and Ahmadi, 2007). Thus, a random-like movement of particles with different velocities occurs that are indicated by the colour bar in fig. 14 for a time of 0.55 s.

A method that recently attracted a large interest is the Immersed Boundary Method (IBM) for particle-laden flows, of which pioneering work was done by Peskin (Peskin, 2002), and therefore,

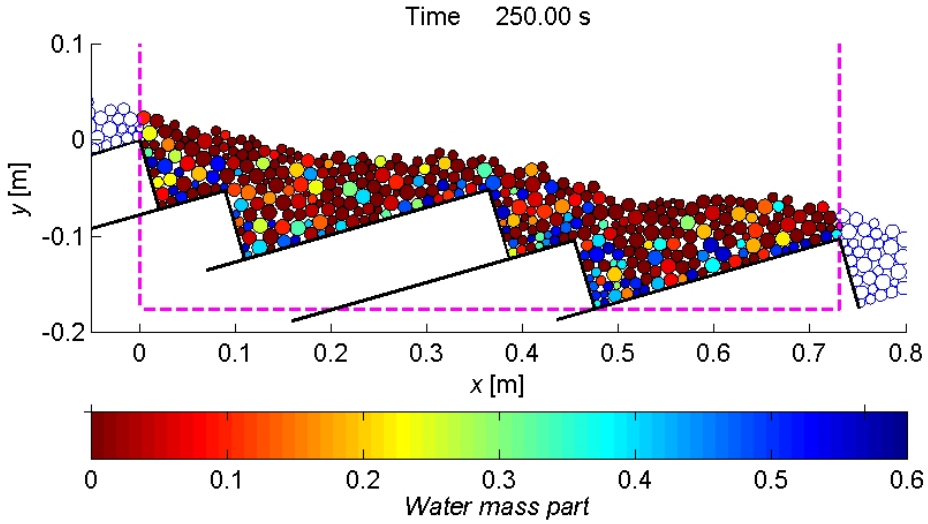

Figure 12: Moisture distribution of individual particles in a moving bed at a time of 250 s

Particle radius (mm)	10
Density (kg/m^3)	400
Young modulus (N)	500000
Poisson ratio	0.45
Friction coefficient	0.8
Coefficient of restitution	0.5
Normal dissipation ($1/s$)	2551.3

Table 3: Mechanical properties of softwood

is not covered in this study. For a detailed description of the approach the reader is also referred to Mittal et al. (Mittal and Iaccarino, 2005) and Wang et al. (Wang et al., 2008) who applied the Immersed Boundary Method to the motion of granular material.

3.4 Granular Media-Structure Interaction

An interaction between granular media and a structure relies on a transfer of forces between them. Granular media consists of an ensemble of particles of which a number of particles may be in contact with a surface e.g. wall. The contact is resolved similar to inter-particle contacts by a representative overlap as shown in fig. 3. It defines the position of impact as well as the force acting on the particle at this position. The same force, however, into the opposite direction defines a mechanical load for the surface. In order to determine the effect of forces on the solid structure, it is discretised by finite elements. The impact of the force is transferred to the nodes of the respective surface element (Bathe, 1996; Zienkiewicz, 1984) and appears as a boundary condition for the finite element system. Hence, integrating particle dynamics and the response of the solid structure due to particle impacts advances both new position of particles and corresponding deformation and stress of the solid structure in time. In order to predict motion of particles accurately, in general a time step of the order of 10^{-5} to 10^{-8} is required. Due to the much higher stiffness of solid

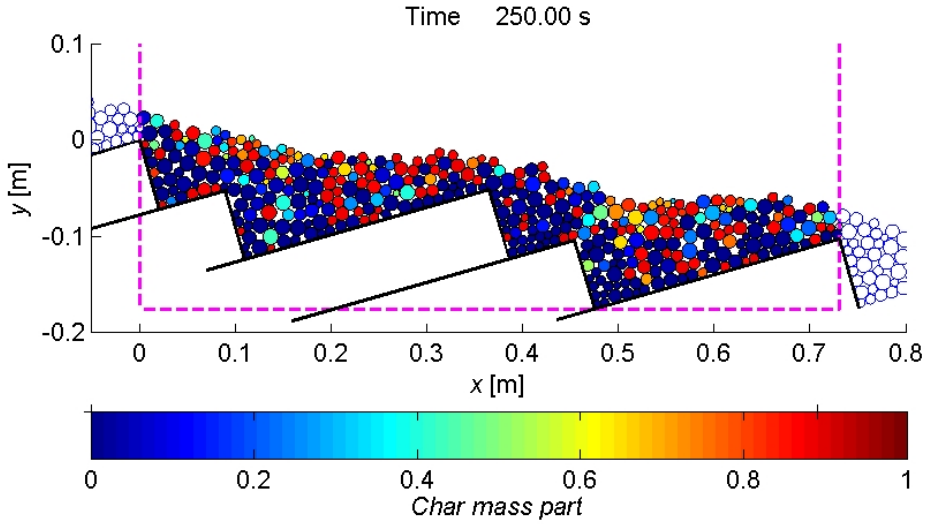

Figure 13: Char distribution of individual particles in a moving bed at a time of 250 s

structures, its deformation during a time step is less than the displacement of particles in contact, so that no numerical instabilities occur.

As a representative example discharge of spherical and cubical particles from a hopper onto a flat surface such as conveyor belt was predicted as depicted in fig. 15.

Under the impact of falling particles the surface deforms as shown in fig. 15 that conversely affects the motion of particles on the surface. Due to an increasing vertical deformation particles roll or slide down toward the bottom of the recess, where they are collected in a heap. Furthermore, during initial impacts deformation waves are predicted, that propagate through the structure, and may, already indicate resonant effects already before a prototype is built.

3.5 Thermo/Mechanical Load

Thermal conversion of solid fuels such as biomass or production of steel in a blast furnace involves heat transfer between heated particles and the bounding walls of the reactor. The heat losses through the walls to the ambient determine the efficiency to a large extent and have been estimated by empirical and integral correlations as summarised by Bird et al. (Bird et al., 1960).

However, a discrete coupling between individual particles and walls as addressed in the current study allows for a more accurate estimate of the heat transferred between particles in contact with a wall and appears as a continuation of interaction between moving and converting particles with a solid structure. Both motion and conversion is described by the Discrete Element Method and the Discrete Particle Method, respectively. The temperature distribution and resulting thermal stress is determined by the Finite Element Method by solving the energy and Navier equations.

The mechanical interaction between granular media a solid structure as described in the previous section detects the position of impact between particles and walls and the respective overlap area. Since particles and walls are assumed to have different temperatures, a heat flux is transferred. The latter depends on the conductivities of both materials and the contact area and is determined similar to particle-particle heat transfer according to eq. 22. The heat flux to the solid structure is treated as an external heat flux over the boundary and consequently appears as a boundary condition for the energy equation. Its solution determines the temperature distribution

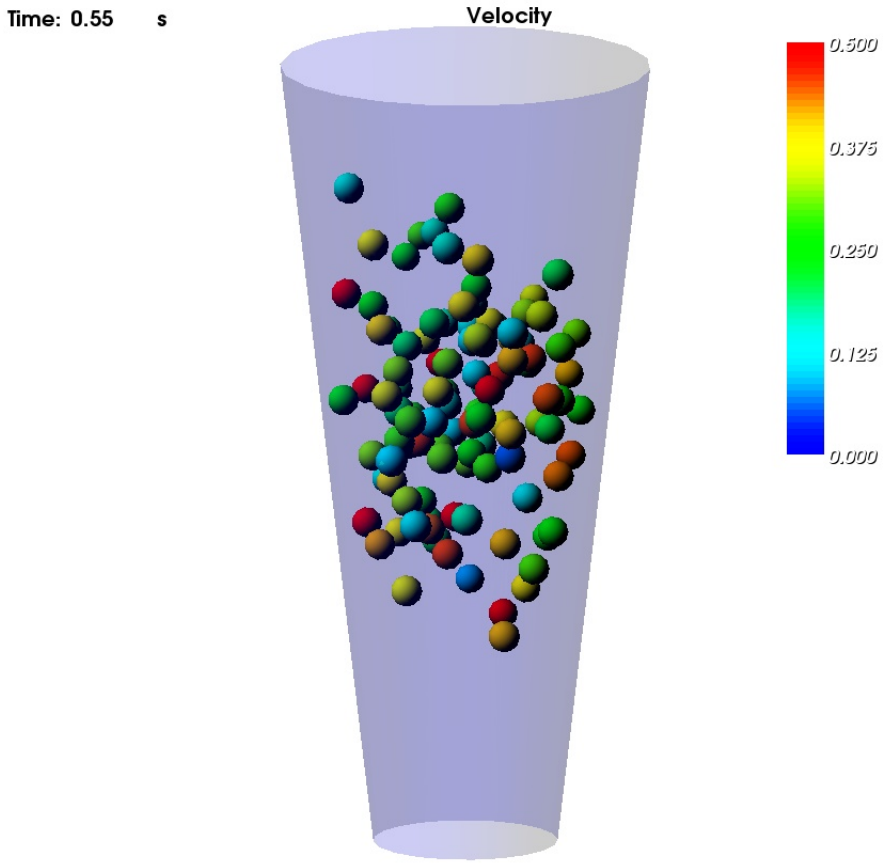

Figure 14: Fluidised bed

within the solid structure.

4 Summary

The current contribution describes the Extended Discrete Element Method (XDEM) as a novel numerical technique to deal with multi-physics applications. It unfolds its predictive capabilities for a coupling between a discrete and a continuous phase. The former describes the motion of particles according to the classical Discrete Element Method (DEM) and extends it by predictions of the thermodynamic state such as temperature or species distribution for individual particles. Particles exchange heat with each other through radiation and conduction when they are in physical contact.

These characteristics are further extended by an interaction with continua by a transfer of heat, mass and momentum between particles and a liquid or gaseous phase and/or solid structures. An arrangement of particles characterised by their position and orientation defines a void space

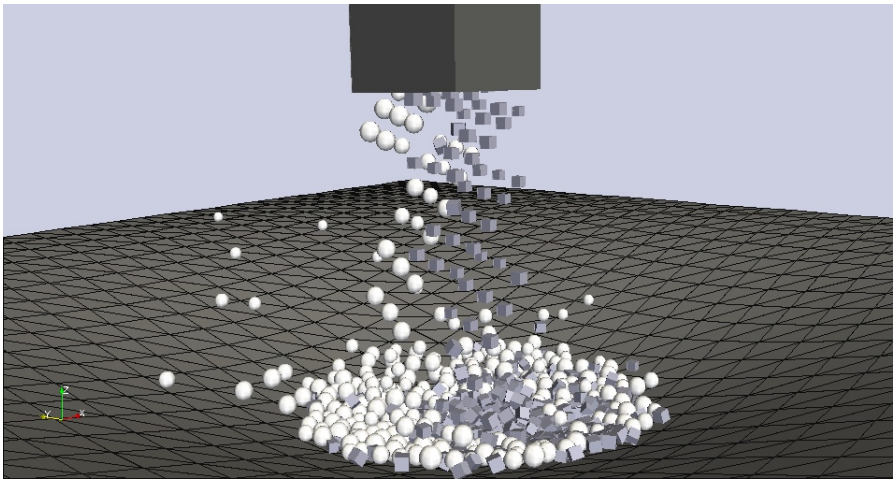

Figure 15: Granular material discharging from a hopper and impinging on a membrane

between them, through which a liquid or gaseous fluid may stream. Thus, locally and time varying distributions of porosity are obtained that influence prevailing flow patterns to a large extend. Accurately predicted flow properties by computational fluid dynamics in conjunction with known surface areas of all individual particles allows evaluating heat and mass transfer with high accuracy. Hence, this novel feature of the presented method omits experimental data or empirical correlations to define both void space and surface area of the solid phase that would be required for a purely based continuous approach. Similarly, impact of particles with solid structures is included in the present method. An impact of particles with a solid structures generates forces at the point of impact that define external loads on the structure. It may be resolved with a finite element method that determines deformation and stress of the solid structure as a response due to particle impacts.

Hence, the Extended Discrete Element Method (XDEM) unfolds its superior predictive capabilities for engineering applications that involve a discrete and continuum phase, for which the interaction between these phases is predicted by the current numerical technique. It allows dealing with a variety of applications that involve both a continuous and a discrete phase. For these applications detailed results are obtained of which an analysis uncovers the underlying physics and leads to improved designs and operating conditions.

A Nomenclature

Physical Symbol	**Meaning**	**Unit**
A	surface	m^2
C	Forchheimer constant	1/m
c	concentration	$kmol/m^3$
c_p	constant-pressure specific heat	W/kg K
c_D	drag coefficient	W/kg K
D	diffusion coefficient	m^2/s
f	correlation coefficient	$-$
F	force	N
$F_{i\rightarrow j}$	view factor	$-$
H_{m}	reaction enthalpy	kJ/kg
h	overlap	m
I	moment of inertia	kgm^2
k	permeability	m^2
M	molecular weight	kg/kmol
m	mass	kg
p	pressure	N/m^2
q	heat flux	W/m^2
r	independent variable	m
S	source term	depending
S_i	inner surface	m^2
t	time	s
T	temperature	K
T_∞	ambient temperature	K
T_{w}	wall temperature	K
$\vec{v}$	velocity	m/s
Y	mass fraction	$-$
Greek Symbol	**Meaning**	**Unit**
α	heat transfer coefficient	W/Km^2
β	mass transfer coefficient	m/s
γ	contact angle	degree
δ	characteristic length	m
Δ	difference	$-$
ϵ	emissivity	$-$
ϵ	porosity	$-$
λ	heat conductivity	W/m^2K
μ	dynamic viscosity	kg/m s
ρ	density	kg/m^3
σ	Boltzmann constant	J/K
τ	tortuosity	$-$
ω	source term	depending
ω	angular velocity	1/s

Dimensionless Number	**Name**
Nu	Nusselt number
Sh	Sherwood number

Subscripts	**Meaning**
eff	effective values
g	gaseous phase
i, j	specie
ij	contact between particle i and j
rad	radiation
s	solid phase
t	tangential direction
x, y, z	coordinate directions
∞	ambient value

Superscripts	**Meaning**
n	geometry exponent

References

P. K. Agarwal. Transport phenomena in multi-particle systems-iv. heat transfer to a large freely moving particle in gas fluidised bed of smaller particles. *Chemical Engineering Science*, 46: 1115–1127, 1991. 2

M. Aho. Pyrolysis and combustion of wood and peat as a single particle and a layer. *VTT Report*, 465, 1987. 8

M. P. Allen and D. J. Tildesley. *Computer Simulation of Liquids*. Claredon Press Oxford, 1990. 6, 11

B.R. Andeen and L.R. Glicksman. Heat transfer to horizontal tubes in shallow fluidised beds. In *ASMEpaper 76-HT-67*, 1976. 2

H.D. Baehr and K. Stephan. *Wärme- und Stoffübertragung*. Springer Verlag, 1. Auflage, Berlin, 1994. 13

S. Balci, T. Dogu, and H. Yücel. Pyrolysis kinetics of lignocellulosic materials. *Ind. Eng. Chem. Res.*, 32:2573–2579, 1993. 15

K. J. Bathe. *Finite Element Procedures*. Prentice Hall, 1996. 3, 5, 20

A. Bejan. *Convection Heat Transfer*. John Wiley & Sons, 1984. 9

R. B. Bird, W. E. Stewart, and E. N. Lightfoot. *Transport Phenomena*. John Wiley & Sons, 1960. 9, 10, 21

R. D. Blevins. *Applied Fluid Dynamics Handbook*. Krieger Publishing Company, Malabar, Florida, 1984. 5, 8

J.S.M. Boterill. *Fluid-bed Heat Transfer*. Academic Press, New York, 1975. 2

J. S. M. Botterill. *Fluid-Bed Heat Transfer*. Academic Press, 1975. 9

H. Brauer. *Stoffaustausch einschließlich chemischer Reaktionen*. Verlag Sauerländer, 1971. 9

J. Bridgewater. *Granular Matter - An Interdisciplinary Apporach*, chapter Mixing and segregation mechanisms in particle flow, pages 161–194. Springer, 1994. 6

C. Canuto, M. Y. HUssaini, A. Quarteroni, and T. A. Zang. *Spectral methods in fluid mechanics*. Springer, Berlin, 1987. 3

W. R. Chan, M. Kelbon, and B. B. Krieger. Modelling and experimental verification of physical and chemical processes during pyrolysis of a large biomass particle. *Fuel*, 64:1505–1513, 1985. 7

P. Chapman. Cfd enhances waste combustion design and modification. In *Combustion Canada '96, Ottawa, Ontario, Canada*, June 5 - 7, 1996. 7

K. W. Chu and A. B. Yu. Numerical simulation of complex particle-fluid flows. *Powder Technology*, 179:104–114, 2008. 2

K. W. Chu, B. Wang, A. B. Yu, A. Vince, G. D. Barnett, and P. J. Barnett. Cfd-dem study of the effect of particle density distribution on the multiphase flow and performance of dense medium cyclone. *Minerals Engineering*, 22:893–909, 2009. 2

A.P. Collier, A.N. Hayhurst, J.L. Richardson, and S.A. Scott. The heat transfer coefficient between a particle and a bed (packed or fluidised) of much larger particles. *Chemical Engineering Science*, 59(21):4613 – 4620, 2004. ISSN 0009-2509. doi: 10.1016/j.ces.2004.07.029. URL `http://www.sciencedirect.com/science/article/pii/S0009250904004658`. 2

C. Crowe, M. Sommerfeld, and Y. Tsuji. *Multiphase Flows with Droplets and Particles*. CRC Press, 1998. 6

C. T. Crowe. On models for turbulence modulation in fluid-particle flows. *International Journal of Multiphase Flow*, 26(5):719–727, 2000. 19

P. A. Cundall and O. D. L. Strack. A discrete numerical model for granular assemblies. *Geotechnique*, 29:47–65, 1979. 6, 11

N. G. Deen, M. V. S. Annaland, M. A. Van Der Hoef, and J. A. M. Kuipers. Review of discrete particle modeling of fluidized beds. *Chemical Engineering Science*, 62:28–44, 2007. 2

F. A. L. Dullien. *Porous Media Fluid Transport and Pore Structure*. Academic Press, San Diego, 1979. 8

Jacques Duran and P.G. De Gennes. *Sands, Powders, and Grains: An Introduction to the Physics of Granular Materials*. Springer, 1999. 6

J. K. Eaton. Two-way coupled turbulence simulations of gas-particle flows using point-particle tracking. *International Journal of Multiphase Flow*, 35(9):792–800, 2009. 19

R. H. Essenhigh, H. E. Klimesh, and D. Förtsch. Combustion characteristics of carbon: Dependence of the zone I-zone II transition temperature (T_c) on particle radius. *Energy and Fuels*, 13:826–831, 1999. 7

Y. Q. Feng and A. B. Yu. Assessment of model formulations in the discrete particle simulation of gas-solid flow. *Industrial & Engineering Chemistry Research*, 43:8378–8390, 2004. 2

Y. Q. Feng and A. B. Yu. An analysis of the chaotic motion of particles of different sizes in a gas fluidized bed. *Particuology*, 6:549–556, 2008. 2

J. H. Ferzinger and M. Peric. *Computation Methods for Fluid Dynamics*. Springer Verlag, Heidelberg, 1996. 3, 5

B. A. Finlayson. *The method of weighted residuals and variational principles*. Academic Press, 1972. 3

J. A. C. Gallas, H. J. Herrmann, and S. Sokolowski. Convection cells in vibrating granular media. *Phys. Rev. Lett.*, 69:1371, 1992. 11

D. Gidaspow. *Multiphase flow and Fluidisation*. Academic Press, 1994. 1

V. Gnielinski. Berechnung des Wärme- und Stoffaustauschs in durchströmten ruhenden Schüttungen. *Verfahrenstechnik*, 16:pp. 36–39, 1982. 13

U. Grigull. *Die Grundgesetze der Wärmeübertragung*. Springer Verlag, 1963. 9

M. Gronli. *A theoretical and experimental study of the thermal degradation of biomass*. PhD thesis, The Norwegian University of Science and Technology Trondheim, 1996. 9, 15

P. K. Haff and B. T. Werner. Computer simulation of the sorting of grains. *Poweder Techn.*, 48: 23, 1986. 11

M. Hellwig. *Zum Abbrand von Holzbrennstoffen unter besonderer Berücksichtigung der zeitlichen Abläufe*. PhD thesis, Technische Universität München, 1988. 7

C. Hirsch. *Numerical Computation of Internal and External Flows*. Wiley & Sons, London, 1991. 3

B. P. B. Hoomans, J. A. M. Kuipers, W. J. Briels, and W. P. M. Van Swaaij. Discrete particle simulation of bubble and slug formation in a two-dimensional gas-fluidized bed: A hard-sphere approach. *Chem. Eng. Sci.*, 51, 1996. 1, 2

http://www.openfoam.com, February 2012. 3

M. Huttunen J. J. Saastamoinen and Richard J.-R. Simultaneous drying and pyrolysis of solid fuel particles. 8

K. D. Kafuia, C. Thornton, and M. J. Adams. Discrete particle-continuum fluid modelling of gas-solid fluidised beds. *Chemical Engineering Science*, 57:2395–2410, 2002. 2

Y. Kaneko, T. Shiojima, and M. Horio. Dem simulation of fluidized beds for gas-phase olefin polymerization. *Chemical Engineering Science*, 54:5809, 1999. 2

E. J. Kansa. A mathematical model of wood pyrolysis. *Combustion and Flame*, 18:238–251, 1972. 15

E. J. Kansa, H. E. Perlee, and R. F. Chaiken. Mathematical model of wood pyrolysis including internal forced convection. *Combustion and Flame*, 29:311–324, 1977. 6, 7

R. D. Kingdon, P. Schofield, and L. White. A lattice boltzmann model for the simulation of fluid flow. *J.Phys. A: Math. Gen.*, 25:3559–3566, 1992. 3

H. Kung. A mathematical model of wood pyrolysis. *Combustion and Flame*, 18:185 – 195, 1972. 15

D. Kunii and O. Levenspiel. *Fluidization Engineering*. Butterworth-Heinemann, 1991. 2

L.D. Landau and E.M. Lifshitz. *Course of Theoretical Physics*. Pergamon Press, 1960. 6

H. P. Langtangen. *Computational Partial Differential Equations: Numerical Methods and Diffpack Programming*. Springer Berlin, 2002. 3, 12

N. M. Laurendeau. Heterogeneous kinetics of coal char gasification and combustion. *Prog. Energy Combust. Sci.*, 4:221, 1978. 7

J. C. Lee, R. A. Yetter, and F. L. Dryer. Transient numerical modelling of carbon ignition and oxidation. *Combustion and Flame*, 101:387–398, 1995. 7

J. C. Lee, R. A. Yetter, and F. L. Dryer. Numerical simulation of laser ignition of an isolated carbon particle in quiescent environment. *Combustion and Flame*, 105:591–599, 1996. 7

J. T. Li and D. J. Mason. A computational investigation of transient heat transfer in pneumatic transport of granular particles. *Powder Technology*, 112:273, 2000. 3

J. T. Li and D. J. Mason. Application of the discrete element modelling in air drying of particulate solids. *Drying Technology*, 20:255, 2002. 3

J. T. Li, D. J. Mason, and A. S. Mujumdar. A numerical study of heat transfer mechanisms in gas-solids flows through pipes using a coupled cfd and dem model. *Drying Technology*, 21:1839, 2003. 3

T. M. Linjewile, A. S. Hull, and P. K. Agarwal. Heat transfer to a large mobile particle in gas-fluidized beds of smaller particles. *Chemical Engineering Science*, 48(21):3671 – 3675, 1993. ISSN 0009-2509. doi: 10.1016/0009-2509(93)81023-O. URL `http://www.sciencedirect.com/science/article/pii/000925099381023O`. 2

K. F. Malone and B. H. Xu. Particle-scale simulation of heat transfer in liquid-fluidised beds. *Powder Technology*, 184:189–204, 2008. 3

Y. H. Man and R. C. Byeong. A numerical study on the combustion of a single carbon particle entrained in a steady flow. *Combustion and Flame*, 97:1–16, 1994. 6

S. Manickavasagam and M. P. Menguc. Effective optical properties of pulverized coal particles determined from FT-IR spectrometer experiments. *Energy Fuels*, 7:860 – 869, 1993. 2

H. S. Mickley and D. F. Fairbanks. Mechanism of heat transfer to fluidised beds. *American Institute of Chemical Engineers Journal*, 1(3):374, 1955. 2

R. Mittal and G. Iaccarino. Immersed boundary methods. *Annu. Rev. Fluid Mech.*, 37:239–261, 2005. 20

H. Nasr and G. Ahmadi. The effect of two-way coupling and inter-particle collisions on turbulence modulation in a vertical channel flow. *International Journal of Heat and Fluid Flow*, 28(6): 1507–1517, 2007. 19

K. Papadikis, S. Gu, and A.V. Bridgwater. Computational modelling of the impact of particle size to the heat transfer coefficient between biomass particles and a fluidised bed. *Fuel Processing Technology*, 91(1):68 – 79, 2010. ISSN 0378-3820. doi: 10.1016/j.fuproc.2009.08.016. URL `http://www.sciencedirect.com/science/article/pii/S0378382009002483`. 2

M. S. Parmar and A. N. Hayhurst. The heat transfer coefficient for a freely moving sphere in a bubbling fluidised bed. *Chemical Engineering Science*, 57(17):3485 – 3494, 2002. ISSN 0009-2509. doi: 10.1016/S0009-2509(02)00259-2. URL `http://www.sciencedirect.com/science/article/pii/S0009250902002592`. 2

S. V. Patankar. *Numerical Heat Transfer and Fluid Flow*. McGraw-Hill Book Company, New York, 1980. 5

C. S. Peskin. The immersed boundary method. *Acta Numerica*, pages 479–517, 2002. 19

B. Peters. Classification of combustion regimes in a packed bed based on the relevant time and length scales. *Combustion and Flame*, 116:297 – 301, 1999. 6, 8

B. Peters. *Thermal Conversion of Solid Fuels*. WIT Press, Southampton, 2003. 12

B. Peters. Numerical simulation of heterogeneous particle combustion accounting for morphological changes. In *27th International Conference on Environmental Systems, Lake Tahoe, USA, SAE-paper 972562*, July 14 - 17, 1997. 8, 9

B. Peters and Ch. Bruch. A flexible and stable numerical method for the decomposition process of wood particles. *Chemosphere*, 42:481–490, 2001. 9

B. Peters and A. Džiugys. An approach to simulate the motion of spherical and non-spherical fuel particles in combustion chambers. *Granular Matter*, 3(4):231–265, 2001. 11

T. Pöschel and T. Schwager. *Computational Granular Dynamics*. Springer Berlin, 2005. 6, 12

W. Prins. *Fluidised bed combustion of a single carbon particle*. PhD thesis, Twente, University, The Netherlands, 1987. 2

W. E. Ranz and W. R. Marshall. Evaporation from drops. *Chemical Engineering Progress*, 48:141, 1952. 3

J. Rattea, F. Mariasb, J. Vaxelaireb, and P. Bernada. Mathematical modelling of slow pyrolysis of a particle of treated wood waste. *Journal of Hazardous Materials*, 170:1023–1040, 2009. 7

P. Richard. Slow relaxation and compaction of granular systems. *Nature Materials*, 4:121128, 2005. 6

J. E. L. Rogers, A. F. Sarofim, J. B. Howard, G. C. Williams, and D.H. Fine. Combustion characteristics of simulated and shredded refuse. *15th Symposium (International) on Combustion*, 15: 1137–1148, 1975. 7

I. B. Ross, M. S. Patel, and J. F. Davidson. The combustion of carbon particles in a fluidised bed. *Transactions of the Institution of Chemical Engineers*, 59:83–88, 1981. 2

P. N. Rowe and A. W. Nienow. Particle mixing and segregation in gas fluidized bedsa review. *Powder Technology*, 15:141–147, 1976. 2

J. Saastamoinen and J.-R. Richard. Simultaneous drying and pyrolysis of solid fuel particles. *Combustion and Flame*, 106:288–300, 1998. 8

J. Saastamoinen, M. Aho, and V.L. Linna. Simultaneous pyrolysis and char combustion. *Fuel*, 72: 599–609, 1993. 8

R. J. Sadus. *Molecular Simulation of Fluids: Theory, Algorithms and Object-Orientation*. Elsevier, 1999. 6

E. U. Schlünder and E. Tsotsas. *Wärmeübertragung in Festbetten, durchmischten Schüttgütern und Wirbelschichten*. G. Thieme Verlag, Stuttgart, 1988. 13

A. Schmidt and U. Renz. Eulerian computation of heat transfer in fluidized beds. *Chemical Engineering Science*, 54(22):5515 – 5522, 1999. ISSN 0009-2509. doi: 10.1016/S0009-2509(99)00298-5. URL `http://www.sciencedirect.com/science/article/pii/S0009250999002985`. 2

A. Schmidt and U. Renz. Numerical prediction of heat transfer in fluidised beds by a kinetic theory of granular flowsnumerical prediction of heat transfer in fluidised beds by a kinetic theory of granular flows. *International Journal of Thermal Sciences*, 39:871–885, 2000. 2

S. Schmidt, J. Büchs, C. Born, and M. Biselli. A new correlation for the wall-to-fluid mass transfer in liquid-solid fluidized beds. *Chemical Engineering Science*, 54(6):829 – 839, 1999. ISSN 0009-2509. doi: 10.1016/S0009-2509(98)00284-X. URL `http://www.sciencedirect.com/science/article/pii/S000925099800284X`. 2

E. Schröder. Bestimmung des Druckverlustes und des Wärmeüberganges von gasdurchströmten Feststoffschüttungen in der PANTHA Anlage. *Bericht Forschungszentrum Karlsruhe*, FZKA 6373, 1999. 15

Pai Shih-I. *Two-Phase Flows*. Vieweg Tracts in Pure and Applied Physics, Braunschweig, 1977. 8

C. Shin and S. Choi. The combustion of simulated waste particles in a fixed bed. *Combustion and Flame*, 121:167–180, 2000. 18

E. Specht. *Kinetik der Abbaureaktionen*. Habilitationsschrift, TU Clausthal-Zellerfeld, 1993. 7, 9

T. Swasdisevi, W. Tanthapanichakoon, T. Charinpanitkul, T. Kawaguchi, and T. Tsuji. Prediction of gas-particle dynamics and heat transfer in a two-dimensional spouted bed. *Advanced Powder Technology*, 16:275, 2005. 3

A. I. Tamarin, D. M. Galerstein, and V. M. Shuklina. Heat transfer and the combustion temperature of coke particles in a fluidised bed. *Journal of Engineering Physics*, 42:14–19, 1982. 2

C. Taylor and T. G. Hughes. *Finite element Programming of the Navier-Stokes equations*. Pineridge Press Limited, 1981. 5

C. L. Tien. Thermal radiation in packed and fluidized beds. *Trans. ASME J. Heat Transfer*, 110: 1230 – 1242, 1988. 2

Y. Tsuji, T. Kawaguchi, and T. Tanaka. Discrete particle simulation of two-dimensional fluidized bed. *Powder Technol.*, 77(79), 1993. 1, 2

O.R. Walton and R.L. Braun. Viscosity, granular-temperature, and stress calculations for shearing assemblies of inelastic, frictional disks. *J. of Rheology*, 30(5):949–980, 1986. 11

C. Y. Wang. *Tramsport Phenomena in Porous Media*, chapter Modelling Multiphase Flow and Transport in Porous Media. Oxford Pergamon, 1998. 2

X. Wang, F. Jiang, J. Lei, J. Wang, S. Wang, X. Xu, and Y. Xiao. A revised drag force model and the application for the gas-solid flow in the high-density circulating fluidized bed. *Applied Thermal Engineering*, 31(14-15):2254–2261, 2011. 3

Z. Wang, J. Fan, and K. Luo. Combined multi-direct forcing and immersed boundary method for simulating flows with moving particles. *International Journal of Multiphase Flow*, 34:283–302, 2008. 20

B. H. Xu and A. B. Yu. Numerical simulation of the gas-solid flow in a fluidized bed by combining discrete particle method with computational fluidd dynamics. *Chemical Engineering Science*, 52:2785, 1997. 1, 2

B. H. Xu and A. B. Yu. Comments on the paper numerical simulation of the gas-solid flow in a fluidized bed by combining discrete particle method with computational fluid dynamics-reply. *Chemical Engineering Science*, 53:2646–2647, 1998. 1

A. B. Yu and B.H. Xu. Particle-scale modelling of gas-solid flow in fluidisation. *Journal of Chemical Technology and Biotechnology*, 78(2-3):111–121, 2003. 2

H. Zhou, G. Flamant, and D. Gauthier. Dem-les of coal combustion in a bubbling fluidized bed. part i: gas-particle turbulent flow structure. *Chemical Engineering Science*, 59:4193, 2004a. 3

H. Zhou, G. Flamant, and D. Gauthier. Dem-les simulation of coal combustion in a bubbling fluidized bed. part ii: coal combustion at the particle level. *Chemical Engineering Science*, 59: 4205, 2004b. 3

H. Zhou, G. Mo, J. Zhao, and K. Cen. Dem-cfd simulation of the particle dispersion in a gas-solid two-phase flow for a fuel-rich/lean burner. *Fuel*, 90:1584–1590, 2011. 2

H. P. Zhu, Z. Y. Zhou, R. Y. Yang, and A. B. Yu. Discrete particle simulation of particulate systems: Theoretical developments. *Chemical Engineering Science*, 62:3378 – 3396, 2007. 1, 2

H. P. Zhu, Z. Y. Zhou, R. Y. Yang, and A. B. Yu. Discrete particle simulation of particulate systems: A review of major applications and findings. *Chemical Engineering Science*, 63:5728–5770, 2008. 1, 2

O. Zienkiewicz. *Methode der Finiten Elemente*. Carl Hanser Verlag, 1984. 3, 5, 20